Baku State University Journal of Earth Sciences & Environment **2025**, v 2 (4), p. 1-11

journal homepage: http://bsuj.bsu.edu.az/en

1D / 2D MODELING FOR INTEGRATED INTERPRETATION OF EM DATA: CASE STUDY PERIKSHKUL, AZERBAIJAN

Avaz L. Mammadov, Ali G. Novruzov

Baku State University, 33, Z. Khalilov str. AZ 1148 Baku, Azerbaijan

https://doi.org/10.30546/209805.2025.2.4.2001

Abstract

In this study, the geological structure of the Perishkul field in Azerbaijan was studied by 1D and 2D modeling of electromagnetic (EM) data. The main goal is to accurately determine the depth and resistivity increase of hydrocarbon-containing (oil-gas) formation. In the 1D inversion stage, the resistivity values of the subsurface layers are determined only as a function of depth (ρ = ρ(z)). Two types of inversion methods were used:Marquardt (Damped Least Squares) and Occam's Smoothness Constraint Inversion.TEM and LOTEM data were interpreted both separately and jointly. A five-layer model was identified in the study area: Layer 1: highly resistive (4–10 Ω m), ~10 m thick; conductive (1–2.5 Ω m), 25–35 m thick; at medium depth (30–800 m), ~4 Ω m; conductive (2–3 Ω m), 4000–6000 m thick; more resistive, approximately 5000–7000 m deep. The increased resistivity of this last layer has been associated with hydrocarbon-bearing geological formation.

Keywords: *1D/2D EM modelling, resistivity variations, inversion modelling, hydrocarbon deposits, mud volcanoes, fluid migration*

*Corresponding author.

E-mail address: avez13@yahoo.com (Avaz L. Mammadov)

ali.novruzov@hotmail.com (Ali G. Novruzov)

1D INVERSION

The first step in interpreting transient EM data is often one-dimensional (1D) inversion, where the resistivity of the model is solely a function of depth (ρ = ρ(z)). The resulting models offer a preliminary understanding of the subsurface resistivity distribution and often provide a sufficient approximation of the true resistivity structure [4].

Applied Inversion Strategy

At the surface of an arbitrary horizontally layered half-space, the EM field components generated by a loop source (TEM) or a dipole source (LOTEM) can be recursively calculated [10]. Different inversion algorithms can then be applied to obtain a model providing a decent fitting between measured and calculated data. The quality of fitting is thereby determined through the root-mean-square error defined as:

$$\mathrm{RMS} = \sqrt{\frac{1}{N}\sum_{i=1}^{N}\frac{(d_{i,meas} - d_{i,calc})^2}{d_{i,meas}^2}} * 100, \qquad (1)$$

where N represents the total number of data points, d_i, measurements represents the ith point of the measured data, and d_i, calculations represents the ith point of the calculated data. In the applied 1D inversion process, two different inversion algorithms were utilized to obtain the best-fit resistivity model: damped least squares [7, 3] and Occam's smoothness constraint inversion [8]. Furthermore, a hybrid global/deterministic approach was used to obtain equivalent models providing a qualitative interpretation of model parameter resolution [13]. In addition to the usual inversion parameters, layer thickness, and layer resistivity, one further parameter, called the calibration factor (CF), is often needed to fit the measured to the calculated data. Hörd [4] and Hörd and Scholl [13] show that shallow geological structures underneath the receivers may distort the measured LOTEM signal. These shallow structures result in a shift of the whole transient to higher or lower voltages. Additionally, receiver misalignment, improper definition of gain, receiver area, topography, current offsets, etc., may also produce this effect. The CF is a scalar value that is multiplied to the synthetic data to provide acceptable fitting between measured and calculated data. Newman [11] concluded that this scaling allows an accurate interpretation of the deeper geological structures. However, near-surface layering will be interpreted incorrectly. Therefore, it is desired to fit the data with a CF close to 1. The data are then solely explained by layer resistivity and layer thickness, making the interpretation less ambiguous. The acquired TEM and LOTEM transients are generally interpreted individually using the 1D inversion approach described above. However, one might also use a joint inversion approach to interpret both data sets simultaneously. The process of joint inversion for geophysical prospecting is explained by Jupp and Vozoff [5]. The idea is to fit data of different geophysical methods to a single resistivity model. This is accomplished by combining the Jacobians into one matrix and the data vector and model functions into individual vectors while keeping the same parameter vector to fit the data. The inversion process stays consistent with the single inversion. However, it should be noted that the forward calculations have to be done separately for each EM method. The combination of both methods generally yields more satisfactory results than either TEM or LOTEM does alone. Additionally, the ambiguity of the inversion result is improved since the number of equivalent models is restricted [6].

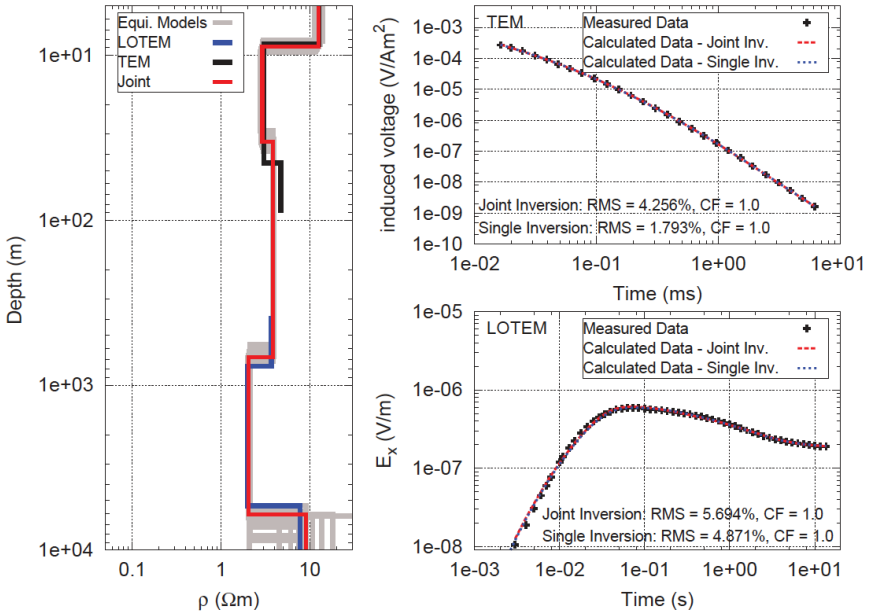

Figure 1. Comparison between TEM and LOTEM single Marquardt inversion models (solid-black and solid-blue lines, respectively) and joint inversion model (red) at Profile A station 01. The equivalent models of the joint inversion are displayed in grey. For both TEM and LOTEM, the data fitting is displayed on the right.

1D Inversion Results The TEM and LOTEM data were individually interpreted using the 1D inversion schemes described above. A full interpretation of the individual 1D inversion models is not conducted in the extent of this publication since the results are fairly similar to the 1D joint inversion. An example is shown in Fig. 1, where a comparison between the individual TEM/LOTEM inversion models (black and blue, respectively) and the joint inversion model (red) obtained at station 01 is displayed. The models are comparable, even though the data fitting of the individual inversion is superior compared with the joint inversion, especially for the TEM transient. However, aside from the upper boundary and resistivity of the third layer (regarding the joint inversion model) at a depth range of 30–800 m, both the joint and individual inversion models suggest a fairly similar subsurface resistivity distribution, at least within the variability of the equivalent models (grey). This behaviour is also valid for the remaining stations. The 1D joint inversion model shown in Fig. 1 is typical for the data obtained in the survey area. Due to the scarce information available for the survey area, the following interpretation is solely based on the resistivity and thickness values provided by the 1D joint inversion and is not correlated with additional borehole data. The subsurface is generally explained by a five-layer model with resistivities ranging between 1 Ω·m and 10 Ω·m. The surface layer is most resistive (4 Ω·m and 10 Ω·m) with a variable thickness of up to 10 m. The second layer is rather conductive with resistivities ranging between 1 and 2.5 Ω·m and a variable thickness of 25–35 m. The third layer extends from approximately 30–800 m and has a resistivity of about 4 Ω·m. The fourth layer is again rather conductive with resistivities ranging from 2–3 Ω·m and a thickness of 4000–6000 m. The resistivity increase of the terminating half-space is presumably the effect caused by the presence of the defined target formation, which may contain possible hydrocarbon deposits. This assumption is based on a geochemical analysis of several selected oil samples in Azerbaijan [1] that lead to the conclusion that most of the oil indeed originates from similar organic facies which are predicted at this depth interval within the survey area. However, based on the strong resistivity variations within the equivalent models, a direct observation of resistivity and depth of this formation is rather doubtful.

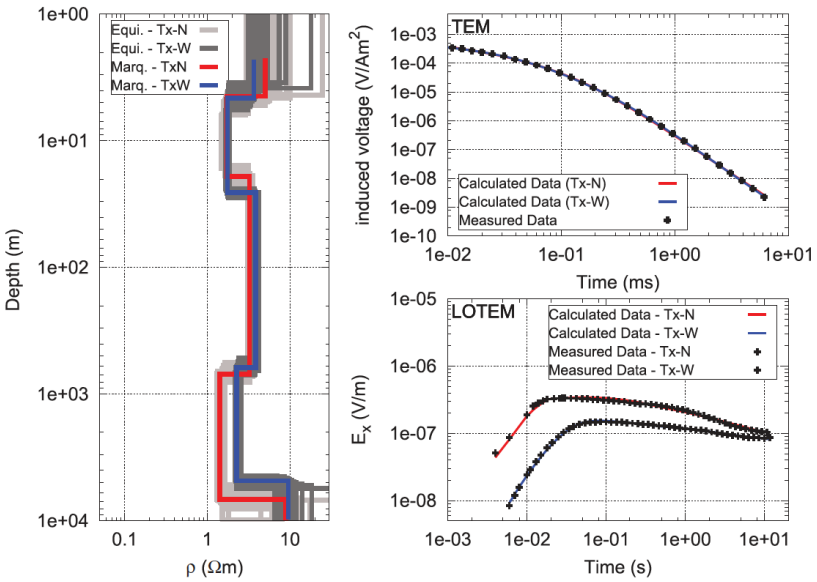

Figure 2. Comparison between the joint Marquardt inversion models obtained at Profile A station 06 from the perpendicular transmitter positions Tx-N (red) and Tx-W (blue). The data fitting of both are displayed on the right.

Figure 2 displays the inversion models at station 06 obtained along Profile A using both transmitter positions Tx-N and Tx-W (red and blue, respectively). The comparison between the inversion models of both transmitter positions obtained at one station is used to investigate possible 2D/3D resistivity structures within the study area. However, based on the results shown in Fig. 2, the subsurface resistivity distribution is predominantly 1D. The models are fairly similar throughout the entire depth range, with the exception of the fourth conductive layer. At this depth, the resistivities of the models are somewhat ambivalent. Nevertheless, compared to the surroundings, this layer still represents a rather conductive layer, and thus, no clear evidence of a 2D/3D resistivity structure could be observed within the survey area. This conclusion is based on the comparison at all other stations that led to a similar result. Consequently, the use of two perpendicular transmitter positions did not lead to definite evidence that the occurrence of the mud volcanoes within the survey area is related to 2D/3D resistivity structures. Presuming a 1D resistivity distribution for large depths within the survey area is consequently justified. One common feature of both models in Fig. 2 is the resistivity increase of the terminating half-space at approximately 5000–6000 m depth. As mentioned, this effect is presumably caused by the presence of the resistive target formation. However, it is noticeable that the variation of the equivalent models increases, implying a poor resolution of the inversion model at this depth. The assumption that this effect may ultimately be an artefact of inversion also seems reasonable. This issue is treated in further modelling studies (see chapter: Modelling Studies). All inversion models obtained along Profile A using Tx-N are displayed in Fig. 2. The topography along the profile and receiver station positions are displayed along the top. Station 01 is thereby the northernmost station, and station 07 is the southernmost. Station 05 is located directly on top of the investigated mud volcano. The inversion models calculated after Occam (green and blue), Marquardt (red), and the equivalent models (grey) are displayed below, labelled 01–07 according to their position along the profile. When jointly inverting TEM and LOTEM data, each transient appeals to a certain minimum and maximum resolvable depth. Generally, it is safe to say that TEM resolves rather shallow resistivity structures (<130 m), whereas LOTEM resolves deeper ones (>200 m for the study area in Azerbaijan). At an intermediate depth range, both methods may either have a certain degree of resolution or no resolution at all. Hence, despite the general agreement between the individual inversion models of both methods (Fig. 6, black

and blue models), it is rather unlikely that they complement each other perfectly. In case of Occam's joint inversion, this may result in oscillations of the resistivity model within this corresponding depth range (see Fig. 8). Although the algorithm generally punishes strong resistivity variations while attempting to fit both data sets simultaneously, it was noticeable that oscillations of the resistivity model occurred at this intermediate depth range at nearly all stations (01, 05, 06, and 07). On the other hand, the individual inversion models show no sign of this behaviour. Consequently, we interpret these oscillations as artefacts of joint inversion and not as actual resistivity variations. Furthermore, it was observable that the oscillation amplitude could be dampened by introducing the CF into the inversion. Especially in case of Marquardt inversion, this was necessary because, otherwise, a further "imaginary layer" would have to be introduced to compensate the resistivity discontinuity.

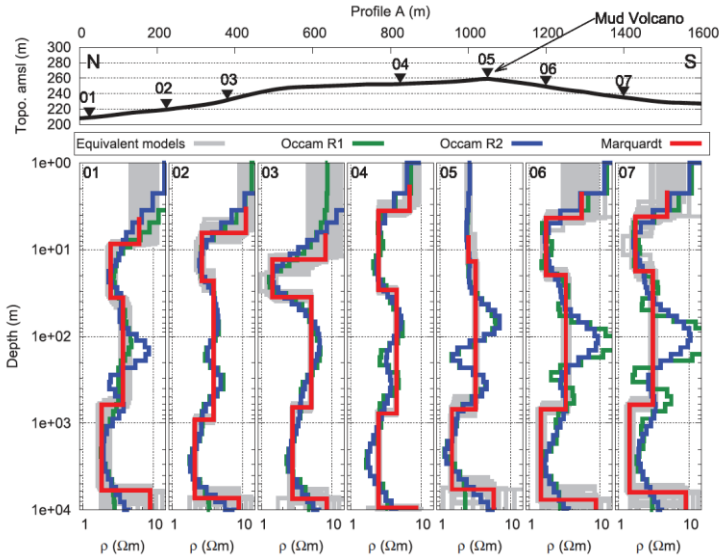

Figure 3. The top image displays the topography along the profile and the receiver positions. The bottom images show 1D joint Occam (green and blue), Marquardt (red) and Monte-Carlo (grey) inversion models of Profile-A utilizing the northern transmitter. The inversion models are arranged according to their positions along the profile. Starting from left (north) to right (south), 01 to 07.

Generally, all inversion models along the profile are fairly similar. Apparent is the interrupted resistive overburden at the mud volcano (station 05). This effect is presumably caused by the increased fluid content of the overburden and presence of shallow mud chambers in the vicinity of the mud volcano. Furthermore, the upper boundary of the third layer seems to have an anticline structure with its maximum at the mud volcano. For deeper regions, the 1D joint inversion models show no indication of a possible 2D resistivity structure, i.e., mud plume or fault structure, along the profile. Considering the variations of the equivalent models, the resistivity distribution of the subsurface at large depths (>200 m) is predominantly 1D since a clear distinction between inversion models of successive stations is not possible. For shallower depths, the applied TEM method could clearly distinguish the location of the mud volcano due to the high resistivity contrast of approximately 1:10 to the overburden. Considering that we obtain an approximate resistivity value of the migrating mud at shallow depths in the vicinity of the mud volcano, we assume that it is also rather conductive at great depths. However, the application of EM methods is only justified if the resistivity of the target object differs significantly from the surrounding media. This is not the case here, and therefore, it is probable that a 2D/3D structure expected to have a rather low resistivity indeed exists within the study area but is not apparent from the EM methods due to the low resistivity contrast with the surrounding media. Also, due to the large

offsets applied in the LOTEM measurements, the method averages over a larger volume of subsurface, resulting in a less focused sensitivity distribution. Small resistivity structures, i.e., mud plumes, may therefore be invisible [9, 12]. The resistivity increase of the terminating half-space is visible in all joint inversion models along the profile. However, similar to before, the resistivity variations of the equivalent models imply that the resistivity possesses a rather poor resolution. This suspicion is validated by the values of the model parameter importance calculated and displayed in Fig. 4(b,c). The resistivity importances displayed in Fig. 4(b) of the terminating half-space are close to zero for all stations implying a poor resolution. Based on these observations, the presence of a resistive terminating half-space is not confirmed. This conclusion is supported by the Eigen parameter (EP) analysis [6] shown in Fig. 4(d), where all EP values are nearly equal to 0 for logρ5. However, considering the importances of the fourth layer and the EP9, an indirect observation of the resistivity increase seems feasible. The model parameter importances, in addition to EP9, indicate that the lower boundary and thickness of the conductive fourth layer are well resolved. Hence, concluding that the presence of the resistive terminating half-space can only be proven based on the presumption that the above lying conductive layer ends at a depth of 5000–7000 m, an additional modelling study seems inevitable to further investigate this issue.

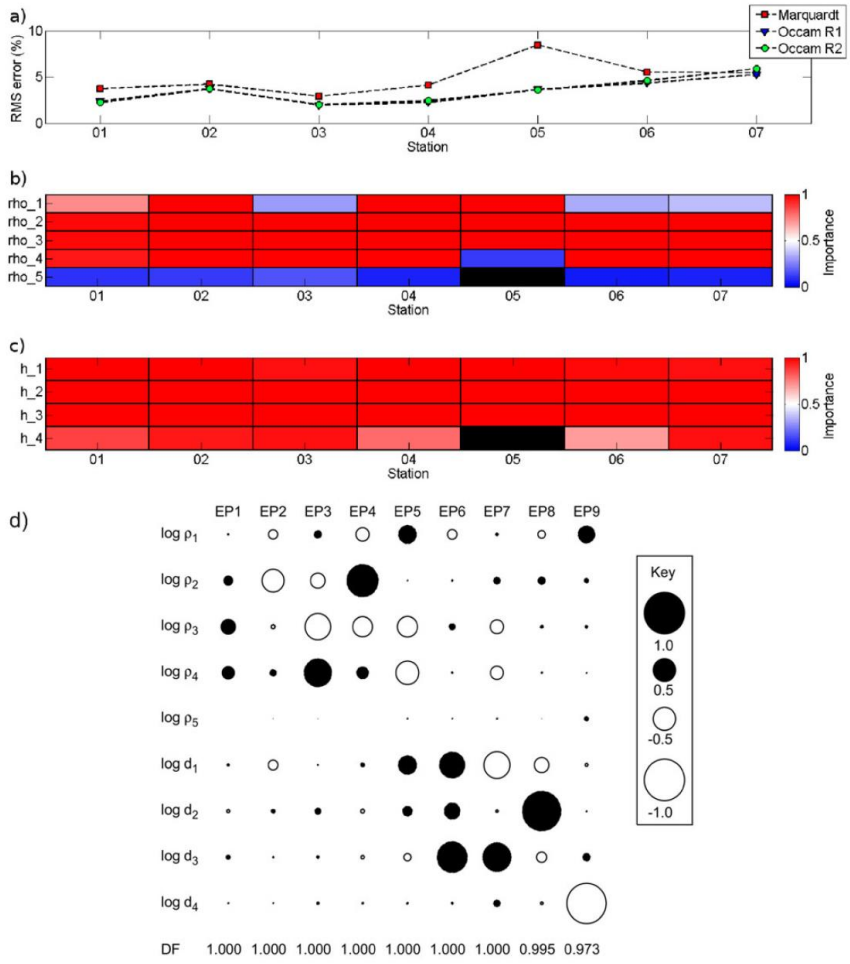

Figure 4. (a) RMS-error of the inversion models at all stations along the profile. (b) and (c) Model parameter importances corresponding to transmitter TxN are displayed. Each importance is represented by a single block of constant colour depending on the importance value of the model parameter. They are arranged according to their position along the profile and depth underneath the surface.

Note that the model of station 05 possesses one layer less due to the absence of the resistive overburden at the mud volcano. (d) Eigen parameters (EPs) and Damping Factors (DF) at the 1.25 percent level for the inversion model obtained at station 01.

MODELLING STUDIES

The 1D joint inversion models suggest a quasi-horizontal layering of the subsurface. The differences between successive inversion models along the profile are generally justified within the variability of the equivalent models. Furthermore, the terminating half-space at a depth of 5000 m to 6000 m is characterized by a resistivity increase for all inversion models along the profile. However, the variability of the equivalent models and, in addition, the model parameter importances and EPs suggest that the resistivity of the terminating half-space is not resolved. Therefore, additional 1D and 2D modelling studies were performed to examine the late-time transient behavior for a given subsurface resistivity distribution.

1D Modelling Study

To analyses the influence of the terminating half-space on the measured LOTEM Ex transients, additional 1D modelling studies were performed. The resistivity and depth of the terminating half-space were varied for each best-fit Marquardt model along Profile A. Subsequently, the RMS errors of the late times (>1 s) were plotted as a function of resistivity and depth. The results for stations 01 and 07 are displayed in Fig. 5. The red horizontal and vertical lines represent the depth and resistivity of the terminating half-space from the best-fit Marquardt model, respectively. The vertical green line represents the resistivity of the fourth layer (e.g., approximately 2 Ωm, see Fig. 3) and is thought as a reference for easier interpretation. The misfit maps of both stations tend to show that the measured data are best explained by a resistive terminating half-space. The RMS error generally increases for all corresponding depths if a conductive (<2 Ωm) terminating half-space was present. Conversely, a minimum RMS value is reached for a resistive terminating half-space located at a depth greater than 4500 m, depending on the resistivity value. This effect is especially prominent at station 01, whereas it is more questionable at station 07. Additionally, the modelling study seems quite ambiguous since the resistivity and depth of the terminating half-space appear to be strongly coupled and are not well resolved due to the large range of equivalent models (white area).

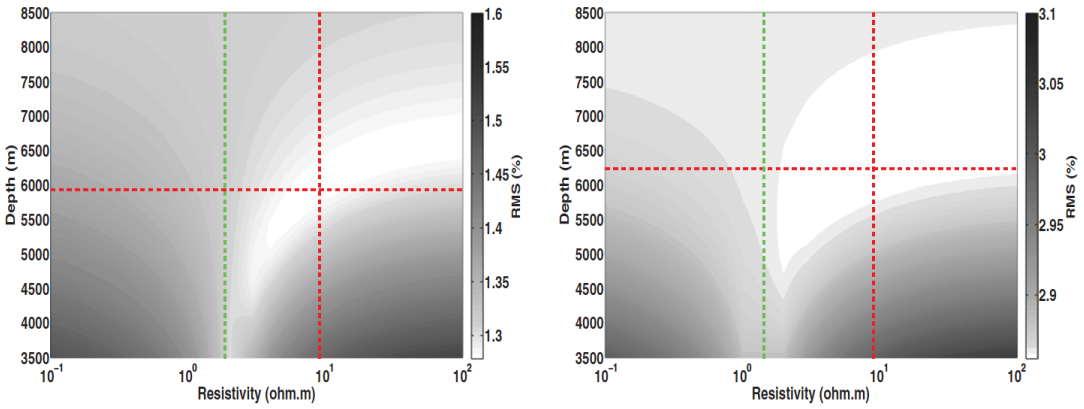

Figure 5. One dimensional modelling study at station 01 (left) and station 07 (right) using LOTEM Ex data. The RMS values are displayed as contours of varying depth and resistivity of the terminating half-space.

Nevertheless, it seems at least reasonable that the lower half-space is more resistive than the overlying conductive layer, even if there is ambiguity in its resistivity and depth. Its presence can generally be

assumed based on the measured LOTEM data, but additional information, such as seismic or borehole data, is needed for a distinct interpretation regarding depth and resistivity.

2D Modelling of LOTEM Ex Transients

To counteract the ambiguity of the 1D modelling study, we attempted to perform a similar investigation by deriving a 2D resistivity model satisfying all measured LOTEM Ex transients simultaneously. It should be mentioned that the TEM transients were not considered for this study. All 2D modelling studies were performed utilizing the 3D forward code sldmem3t [2]. To find the best-fit model, a modified Hedgehog method was applied [4]. The general strategy stipulates that model parameters are defined from the 1D Marquardt inversion models and are varied within a certain interval. The applied procedure varies the model parameters pi in finite steps Δpi between a minimum value p_{min} and a maximum value p_{max}. Synthetic data are calculated for all possible parameter combinations and subsequently compared with the measured data. The minimum fitting is consequently obtained by systematically searching through the model parameter space. Unfortunately, this procedure leads to a large number of models and is computationally expensive for a given number of model parameters and small step sizes. This limitation restricts the extent of the 2D modelling procedure of the Azerbaijan project. For example, the 1D joint inversion Marquardt model consists of five layers (e.g., Fig. 3) meaning nine model parameters are to be determined: five resistivities and four layer thicknesses. Splitting the model space of each parameter into four steps would result in 49 forward calculations. This is not feasible within an appropriate time frame. Therefore, due to the high computational expense, the assembly of a sufficient modelling procedure was restricted.

To consequently limit the extent of the 2D modelling study, shallow regions (<40 m) were grouped into areas with similar resistivities since they are not resolved by the LOTEM Ex data (Fig. 1). The shallow layer boundaries were interpolated along the profile according to the 1D inversion models of TEM. Hence, the nine initial model parameters of the 1D joint inversion were reduced to five: three resistivities and two layer thicknesses. Subsequently, these remaining model parameters were systematically determined by dividing each parameter interval into five steps. The total number of forward calculations reduced to 3125 for each transmitter–receiver configuration. Table 1 summarizes the variations of the model parameters for the 2D modelling study.

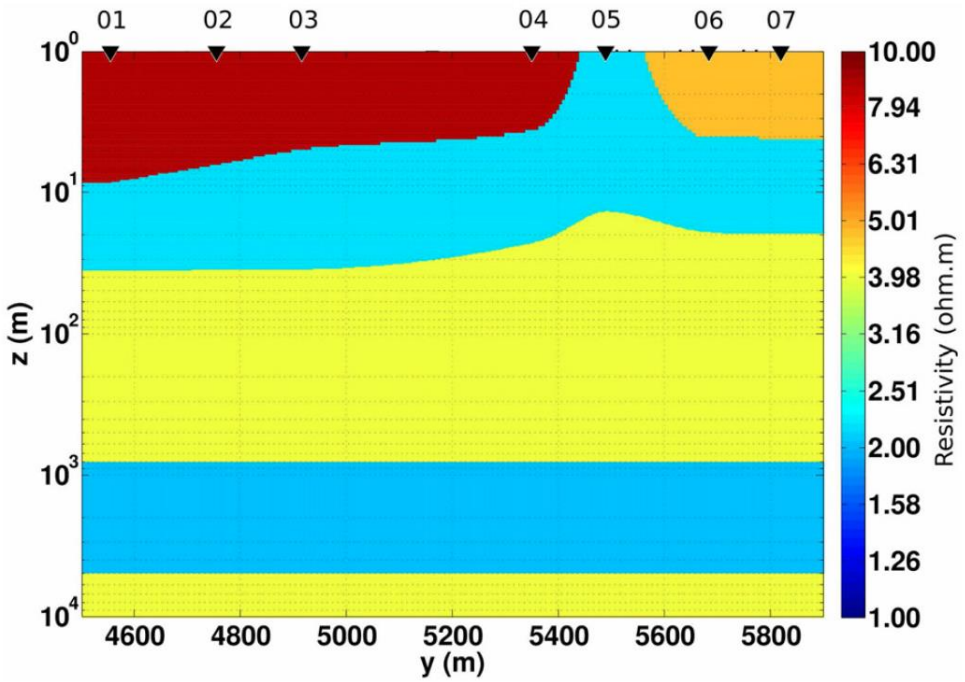

Figure 6. Best-fit model of 3125 forward calculations applying the Hedge-hog method. The positions of the LOTEM Ex stations are marked by black triangles. The mud volcano is situated at station 05.

The best-fit 2D resistivity model of Profile A using the northern transmitter is displayed in Fig. 6. All Ex transients were fitted with a global RMS error of 3.12%. The data fitting at selected stations along Profile A is displayed in Fig. 7. In general, the resistivity distribution is similar to the results of the 1D joint inversion. The terminating half-space has a resistivity of 4 Ωm and starts at a depth of 5000 m, again implying a resistive adjacent half-space. However, as demonstrated by the 1D modelling studies, the resistivity value and depth could also be considerably higher without significantly changing the degree of fitting. Nonetheless, since all LOTEM-Ex transients are best explained by a geological model with a resistive layer at depth, it is the most likely setting.

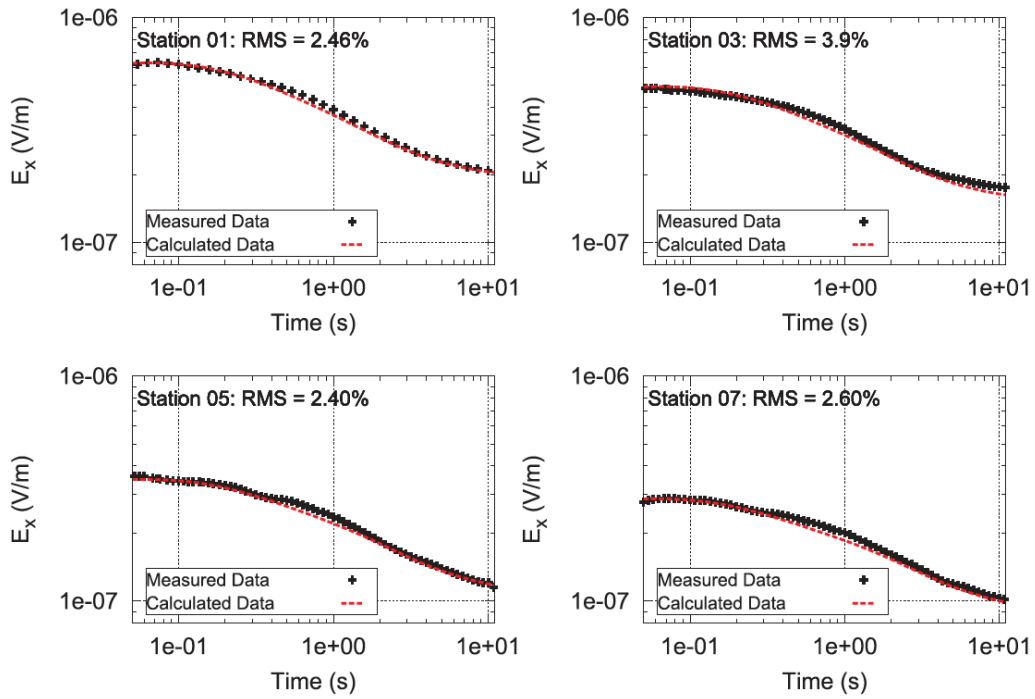

Figure 7. Data fitting of the best-fit 2D resistivity model shown in Fig 11. LOTEM Ex transients at the selected stations 01, 03, 05, and 07 are displayed.

Conclusion:

The aim of the survey was to delineate the depth of a resistivity increase caused by the presence of a hydrocarbon-carrying formation. Indeed, all 1D joint inversion models tend to show a resistive terminating half-space at an approximate depth of 5000-7000 m. However, the model parameter resolution at this depth is very poor, and consequently, the resistivity increase may also be an inversion artefact. Additional 1D/2D modelling studies were performed to investigate the influence of the terminating half-space on the late-time behavior of the measured transients. The results of these modelling studies indicated that a resistivity increase is presumably not the result of an inversion artefact but influenced by the resistive geological formation. However, due to equivalence, the modelling studies also proved that an accurate delineation regarding depth and resistivity of this terminating half-space is not possible. Further geophysical data, i.e., borehole or seismic data, are necessary.

References:

[1] Brunet M.F., Korotaev M., Ershov A.V., Nikishin A.M. 2002. South Caspian Basin Review.

[2] Druskin V.L. and Knizhnerman L.A. 2016. Spectral Approach to Maxwell's Diffusion Equations.

[3] Planke S., Svensen H., Hovland M., Banks D.A., Jamtveit B. 2003. Mud and Fluid Migration in Active Mud Volcanoes.

[4] Hördt A. et al. 1992. Inversion of Long-Offset TEM Soundings.

[5] Jupp D.L.B. and Vozoff K. 2015a. Joint Inversion of Geophysical Data

[6] Jupp D.L.B. and Vozoff K. 2015b. Stable Iterative Methods for the Inversion.

[7] Lange J.O. 2003. Joint Inversion von Central-Loop-TEM und Long-Offset-TEM Transienten.

[8] Milkov A.V. 2009. Worldwide Distribution of Submarine Mud Volcanoes.

[9] Milkov A.V. 2005. Global Distribution of Mud Volcanoes and Their Significance.

[10] Müller M., Hördt A., Neubauer F.M. 2022. Internal Structure of Mount Merapi from Long-Offset TEM Data.

[11] Newman G.A. 2019. Deep Transient Electromagnetic Soundings.

[12] Stewart S.A. and Davies R.J. 2016. Structure and Emplacement of Mud Volcano Systems.

[13] Scholl C. 2017. Influence of Multidimensional Structures on Interpretation of LOTEM Data.